

# Factors Influencing Orientations of Covalently-Attached and Doped Aromatic Groups in Stretched Polyethylene Films

Caihua Wang, Jinqi Xu, and Richard G. Weiss\*

Department of Chemistry, Georgetown University, Washington, D.C. 20057-1227

Received: February 26, 2003; In Final Form: May 16, 2003

Linear polarizations have been measured for covalently attached and doped 9-anthryl and 1-pyrenyl groups residing in interior sites of stretched polyolefinic films. The influences of polymer crystallinity, the concentration of aromatic groups, and the length of the substituents attached to doped molecules or of the tethers to polymer chains of covalently attached species on the degree of polarization have been explored. The results demonstrate the utility of comparing orientational parameters from doped and covalently attached groups in analyzing the factors responsible for stretch-induced orientation. The anthryl and pyrenyl groups prefer to reside in interfacial regions more than amorphous regions even before film stretching, and the specificity of their orientations is determined by the nature of interactions with surrounding polymer chains. The magnitudes of orientation factors are dependent on polymer crystallinity and substituent or tether length, but are independent of aromatic group concentrations as long as they are low. There are significant differences between the orientations of doped and covalently attached groups of the same type due to the inability of the latter to translocate between site types during film stretching. The results, as interpreted in the context of current theories, demonstrate the necessity of crystallite surfaces (i.e., interfacial sites), but not stretching-induced translocation, for selective orientation of aromatic groups along the axis of stretching.

## Introduction

Nearly 70 years ago, Jablonski reported the orientation of small dopant molecules in stretched polymer films, like those of polyethylene (PE).<sup>1</sup> Film stretching involves the interplay between macroscopic (film deformation) and microscopic (partial molecular alignment along defined axes) perturbations. Since the initial report, understanding how alignment occurs has increased enormously, in part as a result of the large number of examples to which the technique has been applied. Models to treat the rapidly expanding body of information include mathematical and physical correlations of molecular shapes<sup>2</sup> with the changes in orientation derived from either vibrational<sup>3</sup> or electronic spectra.<sup>4</sup>

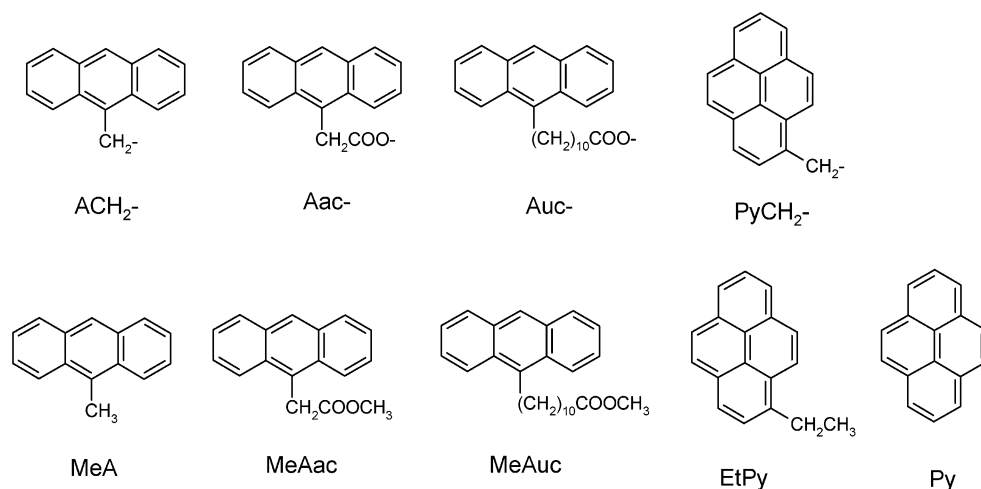
The most popular “shape model” emphasizes the role of molecular shape anisotropy on orientation.<sup>4b,c,5</sup> The “polarizability model” focuses on the electronic interactions between a guest molecule and its host polymer chains.<sup>6</sup> The “epitaxial deposition model” proposes that guest molecules adsorbed on polymer crystal surfaces (i.e., interfacial sites) are responsible for the linear polarization.<sup>7</sup> The “surface tensor model”, also based on molecular shape, emphasizes the need for shape complementarity of a guest and its local environment through minimization of free volume and van der Waals interactions.<sup>8</sup> It is known empirically that the magnitudes of aspect ratios of aromatic dopants and the degree to which they are oriented correlate well only when the molecular shapes are rodlike.<sup>6,8</sup> However, molecular polarizabilities of aromatic molecules of various shapes correlate reasonably well with their orientations.<sup>6</sup> The intrinsic features of the “shape model” and “surface tensor model” seem to be included in the “polarizability model” because the latter considers the balance between repulsive and

attractive intermolecular forces. For that reason, we will discuss these three models as one, the “polarizability/shape model”.

Dopant molecules in *stretched*, partially crystalline polyolefinic films reside both in amorphous regions and on the lateral lamellar faces of crystallites (i.e., interfacial regions),<sup>5,9</sup> but *not* inside the crystalline portions.<sup>7a,c</sup> Stretching destroys spherulitic crystalline aggregates (when they are initially present) while generating networks of microfibrillar crystallite segments whose large lateral crystal surface areas may enhance adsorption of guest molecules and promote their translocation.<sup>7c</sup> Stretching can also increase the degree of crystallinity and the overall degree of orientation of polymer chains in the stretching direction.<sup>7c</sup> According to the “epitaxial deposition model”, a majority of, if not all, dopant molecules reside in the amorphous regions before a film is stretched, and large fractions of the molecules translocate to the crystal surfaces and deposit themselves there epitaxially as a consequence of stretching; the remaining guest molecules in the amorphous regions are not oriented preferentially along the direction of stretching, even though polymer chains surrounding them are to some degree.<sup>7c</sup> This concept was first enunciated by Yogev et al., although at the time they did not realize the importance of interfacial sites and assumed that a fraction of the guest molecules reside inside the crystalline parts.<sup>10</sup>

Chromophores that are covalently attached to polymer chains of polyethylene cannot translocate over a large distance (i.e., most are prohibited from translocating from amorphous regions to crystal surfaces), and yet, they still exhibit nonrandom orientations after stretching. For example, covalently attached 9-anthrylmethyl groups (ACH<sub>2</sub>–) in a low-density polyethylene (LDPE) become aligned preferentially with their long axes along the direction of film stretching, albeit to a smaller degree than the doped 9-methylantracene molecules (MeA) in the same

\* Corresponding author. Phone: 202-687-6013. Fax: 202-687-6209. E-mail: weissr@georgetown.edu.

**SCHEME 1: Structures of Covalently Attached and Doped 9-Anthryl and 1-Pyrenyl Groups and Molecules**

stretched film.<sup>11</sup> This observation raises several questions about the mechanism of alignment:

(1) Is a polymer crystal surface really necessary for chromophore orientation?

(2) If it is, how extensive and how important is molecular translocation from amorphous regions to crystal surfaces during stretching?

(3) Why are covalently attached 9-anthryl groups oriented less well than doped analogues? Is it due to (a) the inability of covalently attached chromophores to translocate from amorphous to interfacial regions when a film is stretched—an explanation consistent with the “epitaxial deposition model”—or (b) conformational constraints imposed by the methylene link of **ACH<sub>2</sub>**—?<sup>11,12</sup>

(4) Finally, how sensitive is the degree of orientation on the type of polyolefin matrix employed?

In an attempt to answer these questions, we have examined the linear dichroic properties of 9-anthryl and 1-pyrenyl groups (Scheme 1) that are either covalently attached to or (non-covalently) doped in interior sites of a series of polyolefinic films of differing chain branching and crystallinity. The results allow the several models for orientation to be examined and the questions above to be addressed.

### Experimental Section

**Instrumentation.** FT-IR spectra were recorded on a MIDAC spectrophotometer. A Varian Mercury 300 MHz NMR spectrometer interfaced to a Sun Sparc station was used to record <sup>1</sup>H NMR spectra (CDCl<sub>3</sub>/TMS). Melting points (corrected) were measured using a Leitz 585 SM-LUX-POL microscope equipped with a Leitz 350 heating stage and an Omega HH21 microprocessor thermometer connected to a K/J thermocouple. HPLC analyses were conducted on an HP series 1100 chromatograph equipped with an autosampler, a silica gel column (IBM, 5 μm, 4.6 × 250 mm) and a diode array detector. A Spex Fluorolog III fluorometer (150 W Osram XBO Xenon lamp) interfaced with a computer was employed for fluorescence measurements. Film crystallinity was determined either by differential scanning calorimetry (DSC) or X-ray diffraction. DSC measurement was done on a Dupont 2910 differential scanning calorimeter that was controlled by a TA module 2000 and data analysis system. X-ray diffraction was measured on a Rigaku R-AXIS image plate system with a Cu Kα source (λ = 1.54056 Å; 46 kV, 46 mA). Data processing and analyses were performed using Materials Data JADE (version 5) XRD software.<sup>13</sup>

**TABLE 1: Some Physical Properties of the Polymer Films Employed**

film	crystallinity <sup>a</sup> (%)		density <sup>e,f</sup> (g/cm <sup>3</sup> )	thickness <sup>f</sup> (μm)
	before stretching	after stretching		
<b>EPDM0</b>	0, <sup>b</sup> 1 <sup>c</sup>	d	0.856	380
<b>EPDM12</b>	12, <sup>b</sup> 12 <sup>c</sup>	d	0.872	380
<b>PE37</b>	37	45	0.900	35
<b>PE46</b>	46	47	0.918	35, 70
<b>PE50</b>	50	58	0.917	25
<b>PE68</b>	68	84	0.945	20
<b>PE74</b>	74	70	0.952	15

<sup>a</sup> From X-ray diffraction measurements unless indicated otherwise.

<sup>b</sup> By differential scanning calorimetry (DSC) measurements. <sup>c</sup> According to supplier. <sup>d</sup> Could not be determined by DSC or X-ray diffraction measurements. <sup>e</sup> As described in ref 14. <sup>f</sup> Before stretching.

Fluorescence decays were determined with an Edinburgh Analytical Instruments model FL900 time-correlated single photon counting system using H<sub>2</sub> as the lamp gas. Films were placed in quartz cuvettes that were either degassed at 10<sup>-4</sup> Torr or flushed with nitrogen and closed with a Teflon cap immediately before use. The film surfaces were at a ca. 45° angle to the exciting beam, and emission was detected at a 45° angle from the back face (a right-angle geometry with respect to excitation and emission). “Instrument response functions” were recorded using Ludox as scatterer. All measurements were performed at ambient temperature. At least 10<sup>4</sup> counts were collected in the peak channel and data were collected over at least 2 decades of decay. Decay histograms were fitted to exponential functions using Edinburgh software supplied with the instrument.

**Materials.** The numbers after the letter acronyms for the polymer films are crystallinities before stretching; crystallinities after stretching, as well as other physical properties, are listed in Table 1. **PE37** (Exxon Exact 3132), **PE46** (Sclair type from Dupont of Canada), **PE50** (Exxon linear low-density PE (LLDPE) 3001.63), **PE68** (type ES-300 from Polialden Petroquimica of Brazil), and **PE74** (Exxon high-density PE (HDPE) 7745.10) were preformed polyethylene films. Prior to use, the **PE** films were immersed in three batches of chloroform for 1 day each to remove antioxidants, plasticizers, and other additives, rinsed with fresh methanol, and dried with a stream of nitrogen. **EPDM0** (Nordel IP 3430 from DuPont-Dow Elastomers; 42.5 wt % ethylene, 57 wt % propylene, 0.5 wt % ethylenenorbornene) and **EPDM12** (Nordel IP 3745 from DuPont-Dow Elastomers; 69 wt % ethylene, 30.5 wt %

propylene, 0.5 wt % ethylenenorbornene) are olefinic copolymers. They were dissolved in 1/1 hexanes/chloroform, precipitated in methanol, dried under vacuum, and pressed into films at ca. 85 °C between two Teflon sheets sandwiched between two glass plates.

Solvents (HPLC grade) were used as received unless indicated otherwise. Dibenzothiophene 5-oxide (**DBTO**), mp 192–194 °C (lit<sup>15</sup> mp 189–191 °C), was synthesized from dibenzothiophene (**DBT**; Aldrich, 95%) as described in the literature.<sup>16</sup> 9-Methylanthracene (99%), mp 79.5–80.5 °C (lit<sup>17</sup> mp 80–81 °C), was purchased from Aldrich. 1-Pyrenecarboxaldehyde (99%) and *p*-toluenesulfonylhydrazide (97%) were from Lancaster and Aldrich, respectively. Pyrene (**PyH**; Aldrich 99%), mp 148.6–149.1 °C (lit<sup>18</sup> mp 149–150 °C), was purified as described.<sup>19</sup> 1-Ethylpyrene (**EtPy**, >99%), mp 95–96 °C (lit<sup>20</sup> mp 94–95 °C), from Molecular Probes was used as received.

**(9-Anthryl)acetyl Chloride.** (9-Anthryl)methanol (Aldrich, 97%) was converted sequentially to 9-bromomethylanthracene,<sup>21</sup> (9-anthryl)acetonitrile, and (9-anthryl)acetic acid.<sup>22</sup> (9-Anthryl)acetyl chloride was prepared from the acid and oxalyl chloride (Aldrich, 98%) in dry benzene at room temperature.<sup>23</sup> <sup>1</sup>H NMR:  $\delta$  (ppm) 5.16 (s, 2H), 7.49–7.64 (m, 4H, Ar), 8.05–8.07 (d,  $J = 8.1$  Hz, 2H, Ar), 8.13–8.15 (d,  $J = 8.4$  Hz, 2H, Ar), 8.52 (s, 1H, Ar). IR (KBr): 1782, 946, 733 cm<sup>-1</sup>.

**Methyl (9-Anthryl)acetate (MeAac).**<sup>24,25</sup> A yellow product (0.1 g; 95%;  $\geq 99\%$  by HPLC), mp 88–90 °C (lit<sup>24</sup> mp 87–88 °C), was obtained from reaction of 0.1 g (0.42 mmol) (9-anthryl)acetic acid, 2.5 mL methanol and 0.1 mL concd sulfuric acid. <sup>1</sup>H NMR:  $\delta$  (ppm) 3.66 (s, 3H, CH<sub>3</sub>), 4.65 (s, 2H, CH<sub>2</sub>), 7.46–7.59 (m, 4H), 8.01–8.04 (d,  $J = 8.4$  Hz, 2H, Ar), 8.26–8.29 (d,  $J = 8.7$  Hz, 2H, Ar), 8.44 (s, 1H, Ar). IR (KBr pellet): 1737, 1202, 1164 cm<sup>-1</sup>. UV/vis (hexanes):  $\lambda_{\max}$  ( $\epsilon$ ) 255 (107700), 317 (1280), 330 (2980), 346 (6240), 364 (9480), 384 nm (8950).

**11-(9-Anthryl)undecanoyl Chloride.** 11-(9-Anthryl)undecanoic acid was synthesized from 9-bromoanthracene using a method adapted from the literature.<sup>26</sup> Under a dry N<sub>2</sub> atmosphere, a solution of 1.0 mL (4.4 mmol) methyl 10-undecenoate (prepared from 10-undecenoic acid chloride (Aldrich, 98%) and methanol) and 8.8 mL (4.4 mmol) 9-borabicyclo[3.3.1]nonane (Aldrich, 0.5 M in THF) was stirred for 3 h. It was transferred to a mixture of 1.03 g (4.0 mmol) 9-bromoanthracene (Aldrich, 94%), 0.098 g (0.12 mmol) [1,1'-bis(diphenylphosphino)ferrocene]dichloropalladium(II) (Aldrich, 1:1 complex with dichloromethane), 4 mL 3 M aqueous sodium hydroxide, and 9 mL THF. After refluxing overnight, the reaction mixture was cooled to room temperature, and water (10 mL) and benzene (25 mL) were added. The mixture was neutralized with 20% hydrochloric acid, and the aqueous phase was extracted with benzene. The combined organic layers were washed with brine and dried over magnesium sulfate. After removal of solvent, purification of the residue by silica gel column chromatography (chloroform as eluant), and recrystallization from acetone and petroleum ether, the yellow acid (41%;  $\geq 97\%$  purity by HPLC analysis), mp 90–92 °C, was obtained. <sup>1</sup>H NMR:  $\delta$  (ppm) 1.30–1.39 (m, 10H, CH<sub>2</sub>), 1.53–1.66 (m, 4H, CH<sub>2</sub>), 1.75–1.83 (m, 2H, CH<sub>2</sub>), 2.33–2.37 (t,  $J = 7.2$  Hz, 2H, CH<sub>2</sub>CO), 3.56–3.62 (t,  $J = 8.1$  Hz, 2H, CH<sub>2</sub>), 7.42–7.53 (m, 4H, Ar), 7.98–8.01 (d,  $J = 8.1$  Hz, 2H, Ar), 8.25–8.27 (d,  $J = 8.7$  Hz, 2H, Ar), 8.32 (s, 1H, Ar). IR (CDCl<sub>3</sub>): 1707 cm<sup>-1</sup>.

The acid was converted to 11-(9-anthryl)undecanoyl chloride using oxalyl chloride.<sup>23</sup> <sup>1</sup>H NMR:  $\delta$  (ppm) 1.28–1.83 (m, 16H, CH<sub>2</sub>), 2.83–2.88 (t,  $J = 7.2$  Hz, 2H, CH<sub>2</sub>CO), 3.55–3.61 (t,  $J = 8.1$  Hz, 2H), 7.41–7.52 (m, 4H, Ar), 7.97–8.00 (d,  $J = 8.4$

Hz, 2H, Ar), 8.24–8.27 (d,  $J = 9.0$  Hz, 2H, Ar), 8.31 (s, 1H, Ar). IR (CDCl<sub>3</sub>): 1799 cm<sup>-1</sup>.

**Methyl 11-(9-Anthryl)undecanoate (MeAuc).** MeAuc was prepared by a method like that for synthesis of 11-(9-anthryl)undecanoic acid, but using sodium methoxide in anhydrous THF instead of aqueous NaOH in THF.<sup>26</sup> After recrystallization from petroleum ether, a white solid (50%; one peak by HPLC analysis), mp 41–43 °C, was obtained. <sup>1</sup>H NMR:  $\delta$  (ppm) 1.30–1.40 (m, 10H, CH<sub>2</sub>), 1.55–1.64 (m, 4H, CH<sub>2</sub>), 1.75–1.86 (m, 2H, CH<sub>2</sub>), 2.28–2.33 (t,  $J = 7.6$  Hz, 2H, CH<sub>2</sub>CO), 3.56–3.62 (t,  $J = 8.1$  Hz, 2H), 3.66 (s, 3H, CH<sub>3</sub>), 7.42–7.53 (m, 4H, Ar), 8.00–8.02 (d,  $J = 8.4$  Hz, 2H, Ar), 8.25–8.28 (d,  $J = 8.7$  Hz, 2H, Ar), 8.325 (s, 1H, Ar). IR (CDCl<sub>3</sub>): 1730 cm<sup>-1</sup>. UV/vis (hexanes):  $\lambda_{\max}$  ( $\epsilon$ ) 331 (2880), 348 (5920), 366 (9380), 387 nm (8760).

**1-Pyrenyldiazomethane.** 1-Pyrenyldiazomethane was prepared from the corresponding hydrazone, which was synthesized from pyrenecarboxaldehyde and *p*-toluenesulfonylhydrazide, following pyrolysis procedures in ethylene glycol as described by Thomas et al.<sup>27</sup> The red and somewhat sticky solid (20% yield), mp 78.0–80.0 °C (dec), was stored as a neat solid at –5 to –10 °C until use. IR (NaCl): 2050 cm<sup>-1</sup>. UV/vis (methanol):  $\lambda_{\max}$  327, 343, 366, and 387 nm.

**Preparation of Polyethylene Films Doped with MeAac (MeAac/PE), MeAuc (MeAuc/PE), Pyrene (PyH/PE), or 1-Ethylpyrene (EtPy/PE).** Acronyms with a slash (/) or a dash (–) represent films with doped (noncovalently attached) guest molecules or with covalently attached groups, respectively. For MeAac and MeAuc, several pieces of 1 cm × 2 cm polyethylene film of the same type were immersed for a few min in a 40 mM chloroform solution of the anthryl molecule. The films were dried in air, dipped quickly in pure chloroform to remove surface-occluded dopants, and thoroughly dried under a stream of dry nitrogen. The average concentrations of imbibed species were calculated from the averaged absorbances of at least three UV/vis absorption spectra (recorded at different positions of each film) and Beers Law, assuming the molar extinction coefficients in a film are the same as those in hexanes. A native film of the same type was used as reference. Similar methods were employed to dope pyrene and 1-ethylpyrene into polyethylene films and to calculate their concentrations.

**Preparation of Polyethylene Films with Covalently Attached 9-Anthryl Groups.** Except for ACH<sub>2</sub>–, which was attached to polyethylene chains by a literature method,<sup>11</sup> 9-anthryl groups were covalently attached to polymer chains of polyethylene films in two steps: film hydroxylation at interior sites followed by esterification with an acid chloride.<sup>28</sup> Typically, a piece of film was immersed in a 0.4 M DBTO/chloroform solution at ca. 40 °C for 24 h, air-dried and rinsed with methanol to remove surface-accessible DBTO, and irradiated (>300 nm) in a Pyrex vial purged with nitrogen. The film was then cleaned as described previously.<sup>28</sup> To prepare films with covalently attached (9-anthryl)acetate groups (**Aac-PE**), four pieces of interior-hydroxylated and one native (i.e., cleaned but neither doped with DBTO nor irradiated) films were immersed in a solution of 0.36 g (1.4 mmol) of freshly prepared (9-anthryl)acetyl chloride, 10 mL of chloroform (Aldrich, 99+%, stabilized with amylene), 70 mg (0.58 mmol) of 4-(dimethylamino)pyridine (Aldrich, 99%), and 10 drops of freshly distilled pyridine. The mixture was stirred under a dry atmosphere for one week at ca. 45 °C. Films were placed in a Soxhlet and extracted with chloroform and hexanes until UV/vis spectra of the last extract showed no evidence of anthryl-containing molecules. Films with attached 11-(9-anthryl)undecanoate groups

(Auc–PE) were prepared by the same method using 11-(9-anthryl)undecanoyl chloride.

The concentration of anthryl groups in each film was calculated as described above for the MeAuc/PE and MeAuc/PE films.

**Preparation of Polyethylene Films with Covalently Attached 1-Pyrenylmethyl Groups (PyCH<sub>2</sub>–PE).** Typically, a 1 cm × 3.5 cm piece of polyethylene film was immersed in a 0.01 M 1-pyrenyldiazomethane/diethyl ether solution at –5 to –10 °C for 24 h, air-dried, rinsed with methanol to remove surface-accessible 1-pyrenyldiazomethane, and irradiated for 10 min at 365 nm (Ultra-Achromatic-Takumar filter, Asahi Optical, Japan; 450 W Hanovia medium-pressure mercury lamp) in a Pyrex vial purged with nitrogen. The irradiated films were immersed in aliquots of diethyl ether until no pyrenyl absorptions were detectable by UV/vis spectroscopy in the last one. Concentrations of attached pyrenyl groups were calculated from UV/vis absorption spectra (averaged from four measurements on different spots of each film) as described above but employing the molar extinction coefficients of 1-ethylpyrene in hexanes as the standard.

**Preparation of Stretched EPDM Films Doped with MeA (MeA/EPDM), MeAuc (MeAuc/EPDM), or Pyrene (PyH/EPDM).** EPDM films (1 cm × 1 cm pieces) were dipped into 1 mM chloroform solution of MeA or MeAuc for a few seconds, dried in air, washed with methanol, and dried with a stream of nitrogen to prepare MeA/EPDM or MeAuc/EPDM films. PyH/EPDM films were prepared by dissolving 1.5 g of EPDM in a refluxing solution of 0.36 mg of pyrene and 50 mL of hexanes over 30 min. The solvent was removed (rotary evaporator followed by vacuum), and the remaining solid was pressed into films as before. EPDM films are elastomers and contract to near their original dimensions if not held in extended form. They were either sandwiched between two tightly clipped quartz glasses, or taped onto a Pyrex glass or cardboard frame with an aperture to allow direct passage of light.

**Measurements of Linearly Polarized Absorption Spectra.** Linearly polarized absorption spectra were recorded at ambient temperature on a Perkin-Elmer Lambda-6 UV/vis spectrophotometer and at low temperature (ca. –30 °C) on a Cary 300 Bio UV/vis spectrophotometer. Films with and without chromophoric groups (vide infra) were cold-stretched by hand to ca. 500% (PE-type), ca. 250–300% (EPDM0), or ca. 400% (EPDM12) of their original length and were mounted vertically (ll) along the stretching direction in the sample and reference compartments, respectively. A Glan-Nicol prism was mounted on each of the sample and reference sides, in front of the films. A background correction was made in the absence of films when the direction of both prisms was vertical (ll) or horizontal (⊥). For the purposes of calculations of optical densities, baselines were corrected empirically to remove the contributions from scatter. Averages of at least three OD<sub>ll</sub>/OD<sub>⊥</sub> (= *d*) ratios from different spots on a film are reported. The 2nd order orientation factor *K<sub>u</sub>* is calculated according to  $K_u = d/(d + 2)$  where *u* is the direction of the transition dipole moment.<sup>4e</sup> In these calculations, we have assumed that the ca. 346 nm peaks of 1-alkylated pyrenes are from pure <sup>1</sup>L<sub>a</sub> transitions, but deviate in the direction of their polarization by a few degrees (vide infra). A homemade sample holder was used for low-temperature measurements. The temperature within the holder was maintained at ca. –30 ± 5 °C by adjusting the rate of a cold and dry nitrogen stream passing continuously through the system.

**Measurements of Linearly Polarized Fluorescence Spectra at Low Temperature.** One Glan-Nicol prism was placed in

the excitation beam and another in the emission beam of the Spex Fluorolog III fluorimeter. Stretched films were mounted vertically (ll) along the stretching direction (defined as *Z*) and normal to the incident light (defined as *X*) in the homemade sample holder mentioned above. Emitted light was collected in a front-face excitation arrangement at an angle of 22.5° (defined as *Y'*; direction *Y* is 90° to both *Z* and *X*) with respect to the incident light beam.

The observed fluorescence intensity is  $I_{UV}(uv)$ , where *U* and *V* represent the polarizing directions of the excitation and the emission light, and *u* and *v* represent the directions of the excitation and the emission transition moment, respectively. The polarizers were placed so that the electric vector of excitation light was polarized along direction *Z* (parallel to the stretching direction) only, and the emitted light was either *Z* or *Y'* polarized. Because stretched PE films are uniaxial, all directions perpendicular to the stretching direction are identical with respect to *Z* (i.e.,  $I_{ZY} = I_{YZ}$ ).<sup>29</sup> The excitation wavelengths for pyrene molecules (338 nm) and 1-pyrenyl groups (346 nm) correspond to absorption transitions along the long molecular axis (*z*) of the chromophores (vide infra), and analyses are based on the  $\gamma$ -emission bands (at 390 nm for pyrene and 392 nm for 1-pyrenyl groups) that correspond to transitions along the *z* molecular axis. Hence, the measurement gives  $I_{ZZ}(zz)$  and  $I_{ZY}(zz)$ . When there is no overlap between *z*- and *y*-polarized spectral features, the 4<sup>th</sup> order orientation factor  $L_{zz}$  can be calculated from the relation,  $I_{ZZ}(zz)/I_{ZY}(zz) = 2L_{zz}/(K_z - L_{zz})$ .<sup>4e</sup> In the case of pyrene and 1-pyrenyl groups, the  $\gamma$ -bands are partially overlapped by *y*-polarized spectral features. Therefore, stepwise spectral reductions were performed (vide infra) to isolate the single-axis polarized components.

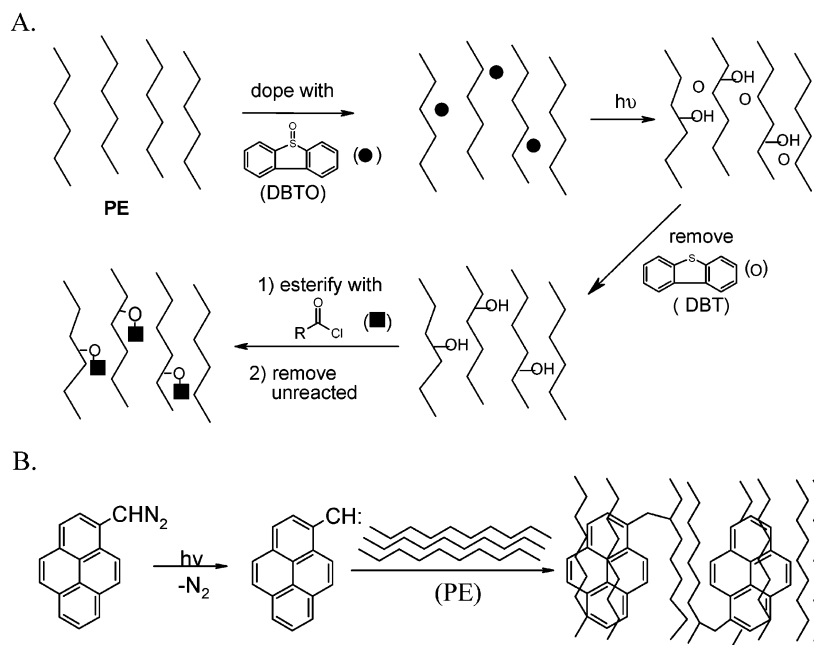
The spectral intensities are not corrected for variations in the flux at different excitation wavelengths, but they are corrected for polarization bias of the instrumental response. To do so, polarized fluorescence spectra ( $\lambda_{ex} = 338$  nm) of pyrene in an unstretched EPDM0 film or dissolved in chloroform were measured at room temperature. In either case, the emission from the pyrene molecules is presumably completely depolarized, and the difference between  $I_{0Z}(zz)$  and  $I_{0Y}(zz)$  (where 0 implies the absence of a polarizer) is the polarization bias in the detector part of the fluorimeter (i.e., including all optical elements in the light path beyond the film). The spectra were corrected as well for baseline excursions by extrapolating the line defined by the emission from 550 to 600 nm (or a wider range) into the shorter wavelength regions and assuming that it represents the true baseline.

**Calculation of Absorption Transition Moments of 1-Methylpyrene (MePy) and 1-Ethylpyrene (EtPy).** After geometry optimization at the PM3 level, electronic (UV/vis) spectra were generated by the ZINDO/S method using a singly excited configuration function. Both programs were a part of the Hyperchem package.<sup>30</sup>

## Results

**Covalent Attachment of 9-Anthryl Groups through Short and Long Alkyl Tethers and 1-Pyrenyl Groups through a Methylene Tether to Polyethylene Chains.** 9-Anthryl and 1-pyrenyl groups were selected as the chromophores for investigation because of their symmetry and well-defined transition dipoles, and because of the existing data from other MeA/LDPE,<sup>5,11</sup> ACH<sub>2</sub>–LDPE,<sup>11</sup> and PyH/LDPE films.<sup>4d</sup> The methods illustrated in Scheme 2 to attach anthryl and pyrenyl groups have been described previously for analogous species.<sup>11,28</sup>

Even films not treated with DBTO could be esterified, albeit to much lower concentrations of anthryl groups (Table 2); the

**SCHEME 2: Cartoon Representation of the Methods for Covalent Attachment of (A) 9-Anthryl and (B) 1-Pyrenyl Groups to Chains in the Amorphous and Interfacial Regions of Polyolefinic Films****TABLE 2: Average Concentrations of Covalently-Attached Anthryl or Pyrenyl Groups in Polyethylene Films**

derivatized film	derivatization agent	attached chromophore concentration <sup>a</sup> (mmol/kg)
Aac-PE46	9-anthrylacetyl chloride	0.6, <sup>b</sup> 3.1 <sup>c</sup>
Auc-PE46	11-(9-anthryl)undecanoyl chloride	0.3, <sup>b</sup> 2.0 <sup>c</sup>
Aac-PE50	9-anthrylacetyl chloride	0.6, <sup>b</sup> 2.4 <sup>c</sup>
Auc-PE50	11-(9-anthryl)undecanoyl chloride	0.6, <sup>b</sup> 2.2 <sup>c</sup>
Aac-PE68	9-anthrylacetyl chloride	0.5 <sup>c</sup>
Aac-PE68	11-(9-anthryl)undecanoyl chloride	0.5 <sup>c</sup>
Auc-PE74	9-anthrylacetyl chloride	0.2, <sup>b</sup> 0.2 <sup>c</sup>
PyCH <sub>2</sub> -PE37	1-pyrenyldiazomethane	2.2
PyCH <sub>2</sub> -PE46	1-pyrenyldiazomethane	3.0
PyCH <sub>2</sub> -PE50	1-pyrenyldiazomethane	3.1
PyCH <sub>2</sub> -PE74	1-pyrenyldiazomethane	2.5

<sup>a</sup> Average values from several films. <sup>b,c</sup> Films derivatized with acid chlorides were esterified either in their native state<sup>b</sup> or after being doped with DBTO and irradiated.<sup>c</sup> (See Experimental Section for details.)

native films must contain hydroxyl groups introduced either at the time of their manufacture or subsequently via autoxidation processes.<sup>31</sup> IR absorption bands from ester groups in some of the modified films containing relatively large amounts of chromophores confirm the presence of ester linkages (e.g., at 1733 cm<sup>-1</sup> in a film with ca. 6.5 mmol Aac groups per kg of PE46). Derivatization of higher crystallinity DBTO-treated polyethylene (e.g., PE74 and PE68) was an order of magnitude less efficient than of lower crystallinity polyethylene (e.g., PE46 and PE50) when the same procedures were employed. In higher crystallinity polyethylene, the concentrations of doped DBTO are smaller than in the films of lower crystallinity because the amorphous fraction of the film (i.e., where DBTO molecules can reside) and the mean hole free volumes are smaller in the former. In addition, there are fewer chain branches and, consequently, fewer easily abstractable tertiary H atoms available to <sup>3</sup>O<sub>p</sub> atoms<sup>32</sup> in the films of higher crystallinity. For these reasons, 9-anthryl concentrations in PE74 and PE68 have greater uncertainties due to their lower UV/vis absorbances and linear polarization measurements were not possible. Rela-

tively low attachment concentrations are sought here to avoid chromophore–chromophore (lumophore–lumophore) interactions.

The course of the 1-pyrenyl attachment process can be followed by UV/vis absorption spectra (Supporting Information Figure 1S). After irradiation and exhaustive washing to remove noncovalently attached pyrenyl species, the characteristic peaks of 1-pyrenyldiazomethane at 366 and 387 nm are replaced by those of a 1-alkylpyrene at 327 and 343 nm.

**Nonpolarized Spectroscopic Properties of Covalently Attached Anthryl and Pyrenyl Groups in Polyethylene Films.** Both the steady-state excitation and emission spectra of unstretched Auc-PE46 are nearly independent of emission and excitation wavelength, respectively (Supporting Information Figure 2S). The time-correlated single photon counting (TCSPC) data from each of the films can be interpreted by a model with only one dominant covalently attached species. Groups attached to different types of sites (i.e., in the interfacial and amorphous regions) are not physically distinguishable directly by these methods or nonpolarized absorption spectroscopy.

Fluorescence decay histograms of unstretched Auc-PE46 and Aac-PE46 films could be fitted well to two decay constants (in addition to a very short scatter component of <1 ns). The longer decay constant,  $\tau_1 \approx 8.9$  ns, is assigned to the loss of excited singlet states of linked 9-anthryl groups. The decay constant reported previously for 9-anthrylmethyl groups covalently attached to polyethylene chains of PE46 is 8.5 ns.<sup>12</sup> The fluorescence decay constants for MeAuc and MeAac doped in unstretched PE46 are ca. 9.4 and 7.4 ns, respectively. The shorter decay constants,  $\tau_s \approx 2.4$ –5.5 ns, in Auc-PE46 and Aac-PE46 are attributed to a fluorophore intrinsic to PE46; they are present in DBTO-treated as well as native PE46 films that have not been esterified. Histograms from unstretched Aac-PE74 and Aac-PE68 were also fitted well to biexponential decays:  $\tau_1 \approx 7.9$  ns from anthryl emissions and  $\tau_s$  from a fluorophore intrinsic to the polymers.

The mole fractions of anthryl groups covalently attached at the different site types are determined at the moment of attachment, and they must remain nearly the same after film

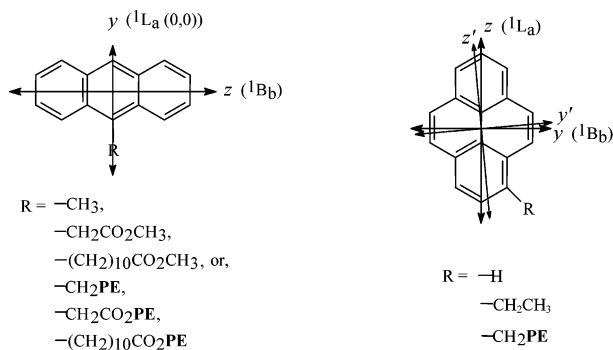


**Figure 1.** Transition dipole directions of 9-anthryl and 1-pyrenyl chromophores. The transition dipole directions in 1-pyrenyl are  $z$  and  $y$  when  $R = -\text{H}$ , and they are  $z'$  and  $y'$  when  $R = -\text{CH}_2\text{PE}$  or  $-\text{CH}_2\text{CH}_3$ .

stretching. When an **Aac-PE46** film was stretched and examined by the TCSPC technique, the fluorescence decay constant from the anthryl groups was 8.4 ns (in addition to that from the fluorescent impurity intrinsic to the polymer, 4.6 ns), near the value obtained before film stretching. Changes in the environment of the chromophores caused by stretching were negligible within the sensitivity of this technique.

Histograms from both **PyCH<sub>2</sub>-PE50** and **PyCH<sub>2</sub>-PE46** could be fitted to a decay constant of ca. 200 ns that constituted ca. 98% of the total. The dominant (88–93%) decay constants of **PyCH<sub>2</sub>-PE37** and **PyCH<sub>2</sub>-PE74**,  $\tau_1$ , are also near 200 ns. Histograms from each film also have a shorter decay constant,  $\tau_s \approx 35$ –82 ns, which may be from a non-pyrenyl species produced during UV irradiation of the precursor; it is not from a pyrenyl excimer, based on fluorescence spectra. Because the decay constants reported for **EtPy/PE46** and **EtPy/PE68** are ca. 200 ns,<sup>33</sup> the emitting species responsible for this decay in the films treated with 1-pyrenyldiazomethane is almost certainly 1-pyrenyl as well.

The ratio of the intensities of the (0,0) emission band and either the (0,1) or (0,2) emission band from **Auc-PE46** (Figure 2S) containing  $2 \times 10^{-3}$  mol/kg **Auc-** groups is much lower than that from  $10^{-5}$  M **MeAuc** in hexanes (spectra not shown) or  $10^{-5}$  mol/kg **ACH<sub>2</sub>-** groups covalently attached to **PE46**.<sup>12</sup> Radiative energy transfer<sup>34</sup> among anthryl groups of **Auc-PE46**, the apparent reason for the low emission ratio, should not occur at a  $2 \times 10^{-3}$  mol/kg anthryl concentration unless the lumophores are not distributed evenly within the noncrystalline regions of the films. Strong evidence for irregular distributions (but not aggregation) of relatively low concentrations of molecules in the noncrystalline regions of other polyolefinic films has been obtained.<sup>33</sup>

**Orientations of Covalently Attached Anthryl and Pyrenyl Groups or Doped Anthryl- and Pyrenyl-Containing Molecules in Stretched Polyolefinic Films.** The orientation factors  $K_z$  of 9-anthryl and 1-pyrenyl groups in stretched polyolefinic films, as well as pertinent literature values, are collected in Tables 3 and 4. For biaxial molecules such as anthracene or pyrene in a uniaxial system like stretched polyethylene,  $K_u = \langle \cos^2(u, Z) \rangle$  where  $u$  and  $Z$  are, respectively, the directions of the transition dipole moment and the stretching of film, and  $(u, Z)$  represents the angle between them.<sup>4c</sup> The  $^1\text{B}_b$  transition of anthracene (ca. 260 nm) is polarized along its long molecular axis (designated as  $z$ ) and the  $^1\text{L}_a(0,0)$  band (ca. 390 nm) is polarized along the short, in-plane molecular axis (designated as  $y$ ) (Figure 1). Conformational effects from 9-alkyl substituents of anthracene only weakly perturb the orbital-pairing symmetry and do not change the directions of these transition moments.<sup>35</sup>

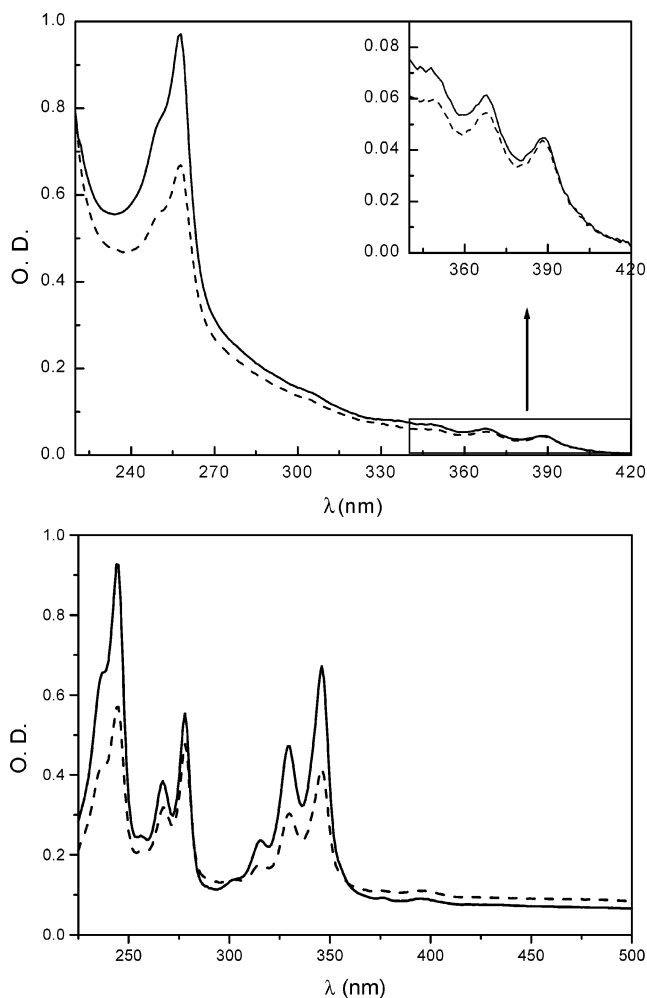


**Figure 2.** Linearly polarized absorption spectra of ca.  $5 \times$  stretched (top) **Aac-PE46** ([anthryl]  $\approx 3.1$  mmol/kg) with the long wavelength region expanded in the inset and (bottom) **PyCH<sub>2</sub>-PE46** ([PyCH<sub>2</sub>-]  $\approx 3.0$  mmol/kg). Baseline-uncorrected  $\text{OD}_{\parallel}$  —;  $\text{OD}_{\perp}$  - - -.

Due to the weakness of the absorbances of the films at ca. 390 nm (Figure 2), the experimental errors associated with  $K_y$  are large. Therefore, discussion of linear polarizations of anthryl groups will be based only upon  $K_z$  values (i.e., from  $^1\text{B}_b$  transitions). The larger the value of  $K_z$ , the better aligned is the long molecular axis of the anthryl groups along the stretching direction.

Both the  $^1\text{B}_a$  (ca. 244 nm) and  $^1\text{L}_a$  (ca. 339 nm) transitions of pyrene are polarized along the long molecular axis ( $z$ ); the  $^1\text{B}_b$  transition (ca. 278 nm) is polarized along the short, in-plane molecular axis ( $y$ ).<sup>4c</sup> Calculations of the transition dipoles of **MePy** and **EtPy** indicate that an alkyl substituent at the 1-position of pyrene causes a deviation of the  $z$  and  $y$  in-plane transition moments from the short and long molecular axes by 4–5° (Figure 1), and a red-shift of the  $^1\text{L}_a$  transition to 346 nm (Figure 2). The orientation factors  $K_z$  of pyrene and 1-substituted pyrenyl groups (including the covalently attached ones) reported in Table 4 were calculated from absorbances at ca. 339 and 346 nm, respectively. Therefore,  $K_z$  of pyrene refers to the orientation of its  $z$  molecular axis in the direction of film stretching, and  $K_z$  of the 1-pyrenyl groups refers to the orientation of their  $z'$  axis with respect to the stretching direction (Figure 1). We note that the deviation in the directions of transition dipoles caused by a 1-alkyl substituent on pyrene is analogous to the Ham effect<sup>36</sup> that is caused by anisotropic solvent interactions.<sup>4d</sup>

**TABLE 3: Orientation Factors ( $K_z$ ) of 9-Anthryl Groups in Stretched PE and EPDM Films at Room Temperature (RT) and  $-30\text{ }^\circ\text{C}$** 

sample <sup>a</sup>	[anthryl] (mmol/kg)	$K_z$ (RT) <sup>b</sup>	[anthryl] (mmol/kg)	$K_z$ ( $-30\text{ }^\circ\text{C}$ ) <sup>b</sup>
MeA/EPDM0	0.3	0.33	0.1	0.32
MeAuc/EPDM0	0.1	0.34		
MeA/EPDM12	0.1	0.42	0.1	0.49
MeAuc/EPDM12	0.1	0.40		
MeAac/PE37	0.3	0.52	0.3	0.60
	1.4	0.51	1.4	0.61
MeAuc/PE37	0.1	0.46	0.1	0.49
	0.5	0.44	0.5	0.46
MeA/PE46 <sup>d</sup>	0.7	0.58		
MeAac/PE46	0.4	0.60	0.4	0.68
	1.9	0.58		
	3.1	0.58		
MeAuc/PE46	0.6	0.49	0.6	0.51
	0.3	0.45		
	2.6	0.45		
	8.5	0.44		
ACH <sub>2</sub> -PE46 <sup>d</sup>	0.4	0.49		
Aac-PE46	0.6 <sup>e</sup>	0.47	0.6	0.49
	3.1	0.47		
Auc-PE46	0.3 <sup>e</sup>	0.45	0.3	0.48
	1.4	0.45		
MeAac/PE50	0.3	0.58	0.3	0.68
	2.3	0.54		
	4.4	0.56		
MeAuc/PE50	1.2	0.47	1.2	0.49
	3.8	0.45		
	5.9	0.44		
Aac-PE50	0.6 <sup>e</sup>	0.50	0.6	0.52
	2.4	0.49		
Auc-PE50	0.6 <sup>e</sup>	0.51	0.6	0.54
	2.2	0.47		
ACH <sub>2</sub> -PE50	0.4	0.46	0.4	0.47
MeAac/PE68	0.5	0.59	0.5	0.60
	0.6	0.57		
	2.5	0.59		
MeAuc/PE68	0.5	0.46	0.5	0.46
	2.6	0.46		
	4.1	0.48		
MeAac/PE74	1.5	0.58	1.5	0.60
	1.2	0.57		
	2.8	0.58		
MeAuc/PE74	1.0	0.46	1.0	0.48
	2.4	0.49		
	3.5	0.46		

<sup>a</sup> All esterified films were pretreated by DBTO-doping and irradiation unless specified otherwise. <sup>b</sup>  $\pm 0.02$ . <sup>c</sup>  $\pm 5\text{ }^\circ\text{C}$ . <sup>d</sup> Ref 11. <sup>e</sup> Esterified without pretreatment by DBTO-doping or irradiation.

**9-Anthryl-Containing Molecules (MeA and MeAuc) or Pyrene (PyH) Doped in EPDM0, a Nearly Completely Amorphous Polyolefin.** Infrared dichroic measurements on a cross-linked ethylene-propylene rubber doped with acridine support the "epitaxial deposition model", which predicts that aromatic molecules are not oriented in amorphous regions of the "rubbery state" of a stretched polyethylene film, although polymer chains surrounding the dopants may be somewhat oriented in the stretching direction.<sup>7c</sup> To the best of our knowledge, no other experiments have tested this prediction directly. However, indirect evidence, based on the spectroscopic properties of a polyethylene matrix, have led others to the same conclusion as found here.<sup>29</sup>

The composition (ethylene, propylene, and 0.5 wt % of ethylenenorbornene) and morphology ( $\leq$ ThinSpace1% crystallinity) of EPDM0 make it an excellent model for a completely amorphous polyolefin (i.e., one that lacks interfacial regions). Consistent with this model, no net orientation was detected from stretched films of EPDM0 films containing either doped MeA,

**TABLE 4: Orientation Factors ( $K_z$ )<sup>a</sup> of Pyrenyl Groups in Stretched PE and EPDM Films**

sample	[Py] (mmol/kg)	$K_z$ (RT)	[Py] (mmol/kg)	$K_z$ ( $-30\text{ }^\circ\text{C}$ ) <sup>b</sup>
PyH/EPDM0	1.0	0.34	0.7	0.33
PyH/EPDM12	0.3	0.40	0.3	0.46
PyH/PE37	5.0	0.48	6.5	0.49
PyH/PE46	3.8	0.50	2.0	0.52
PyH/PE68	5.7	0.55	1.0	0.57
PyH/PE74	8.5	0.55	1.2	0.58
EtPy/PE37	12.5	0.53	2.4	0.55
EtPy/PE46	3.0	0.51	4.0	0.55
EtPy/PE46	0.6	0.56	0.4	0.61
EtPy/PE46	1.8	0.57	1.0	0.61
EtPy/PE74	3.9	0.55	2.7	0.59
PyCH <sub>2</sub> -PE37	2.2	0.44	2.2	0.45
PyCH <sub>2</sub> -PE46	3.0	0.47	3.0	0.48
PyCH <sub>2</sub> -PE50	3.1	0.47	3.1	0.51
PyCH <sub>2</sub> -PE74	2.5	0.49	2.5	0.51

<sup>a</sup>  $\pm 0.02$ . <sup>b</sup>  $\pm 5.0\text{ }^\circ\text{C}$ .

MeAuc or PyH (Tables 3 and 4); in all cases,  $K_z \approx 0.33$ . Molecules associated with interfacial regions appear to be the sole source of linear polarization in stretched polyethylenes.

**Doped Anthryl Molecules with Short (MeA, MeAac) and Long (MeAuc) 9-Substituents.** Generally, MeAac is oriented better than MeAuc in our stretched polyethylene films. For instance, at room temperature,  $K_z \approx 0.58$  for MeAac/PE46, MeAac/PE50, MeAac/PE68, and MeAac/PE74 while  $K_z \approx 0.45$  for MeAuc/PE46, MeAuc/PE50, MeAuc/PE68, and MeAuc/PE74 (Table 3). In PE37,  $K_z \approx 0.52$  for MeAac and 0.45 for MeAuc (Table 3). The difference between the two values is far outside the limits of our estimated experimental error ( $\pm 0.02$ ) for  $K_z$  on the basis of results from several films of the same type containing the same chromophores, and the differences become more pronounced at the lower temperatures (vide infra).

The MeAac/PE46 value is the same as that reported previously for MeA in PE46.<sup>11</sup> MeAac and MeAuc are both free to translocate from amorphous regions to crystal surfaces during film stretching. They differ only in the length of the substituent at the 9-position (Scheme 1). Since MeAuc is oriented less well than MeAac in all of the films, interactions between the anthryl substituent and nearby polyethylene chains must contribute to the overall molecular alignments. Also, the difference between the  $K_z$  values of MeAac and MeAuc in PE37 is smaller than in more crystalline stretched PE films (PE46-PE74). In an even lower crystallinity stretched film, EPDM12, the difference between the  $K_z$  values of doped MeA and MeAuc is only 0.02 (within the limit of experimental error). When in a stretched film with virtually no crystalline regions, like EPDM0, the 9-anthryl molecules with both short (MeA) and long (MeAuc) substituent chains are randomly oriented ( $K_z \approx 0.33$ ). The several ways that film crystallinity manifests itself in chromophore orientation will be treated in subsequent discussions.

**Covalently Attached 9-Anthryl Groups with Short and Long Tethers.** Unlike the orientational differences noted among the three noncovalently attached anthryl molecules, the average orientations of 9-anthryl groups covalently attached to PE through a methylene, an acetate, or an undecanoate tether are the same within experimental error at room temperature:  $K_z = 0.47 \pm 0.02$  for ACH<sub>2</sub>-PE50, Aac-PE50, Auc-PE50, ACH<sub>2</sub>-PE46, Aac-PE46, and Auc-PE46 (Table 3). We anticipated that tethers of longer lengths would provide more rotational freedom and produce higher average orientations if chromophore orientation is influenced strongly by conforma-

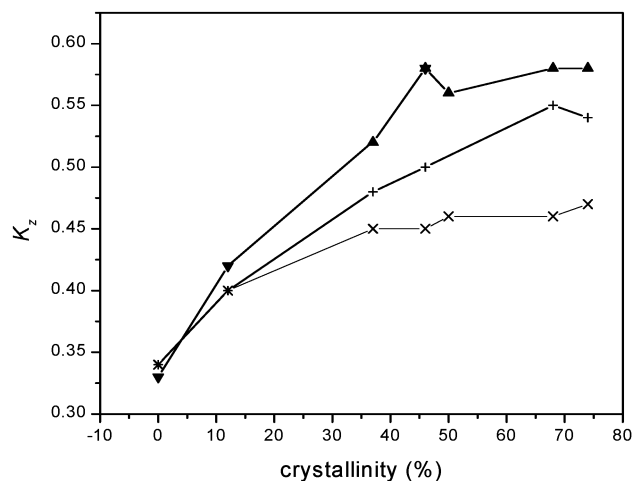


**Figure 3.** Room-temperature orientation factors,  $K_z$ , of **MeA** ( $\nabla$ ), **MeAac** ( $\blacktriangle$ ), **MeAuc** ( $\times$ ), and **PyH** (+) in stretched polyethylene films of different crystallinities versus percent crystallinity.

tional constraints imposed by the tether. The data obtained indicate that this is not so. Regardless of the length of the tether, the 9-anthryl groups sense their environment to a similar degree and are oriented accordingly. Due to strong favorable van der Waals interactions, the long alkyl tether of the **Auc** group should prefer to align parallel to neighboring polymer chains. As a result, the long tethers may provide no more orientational freedom to the anthryl groups than the shorter linkages.

#### Covalently and Noncovalently Attached Pyrenyl Groups.

Similar to results obtained with 9-anthryl groups with short substituents, orientations of doped 1-ethylpyrene molecules are larger than those of covalently attached 1-pyrenylmethyl groups at room temperature (Table 4):  $K_z = 0.51$ – $0.57$  from **EtPy/PE37**, **EtPy/PE46**, and **EtPy/PE74** and  $0.44$ – $0.49$  from **PyCH<sub>2</sub>-PE37**, **PyCH<sub>2</sub>-PE50**, **PyCH<sub>2</sub>-PE46**, and **PyCH<sub>2</sub>-PE74**. We had expected  $K_z$  from the stretched **PyH/PE** films to be higher than or similar to those of stretched **EtPy/PE** because the biaxial symmetry of pyrene is not disturbed by an off-axis substituent. However,  $K_z(\text{EtPy}) \geq K_z(\text{PyH})$  consistently.

Calculations of interaction energies using the “polarizability/shape model”<sup>37</sup> indicate four stable orientations for pyrene molecules on **PE** crystallite surfaces. Their weighted average, as well as the fraction of pyrene molecules residing in the amorphous regions, determine the observed dichroism.<sup>37</sup> The ethyl group of **EtPy** must induce small orientational changes on the crystallite surfaces and/or their distributions that may allow the pyrenyl  $z'$  axis, on average, to become more parallel to the direction of film stretching than the  $z$  axis of pyrene.

**Effects of Chromophore Concentration and Polyethylene Crystallinity on Chromophore Orientation.** The orientation factors at room temperature are invariant within the limited chromophore concentration range investigated (Tables 3 and 4). Over the widest range explored,  $0.3$ – $8.5$  mmol/kg,  $K_z$  of **MeAuc/PE46** remained ca.  $0.45$ . These results suggest that aromatic dopant molecules have a very strong preference for sites in interfacial regions in stretched films, and that these sites are not saturated in the concentration ranges investigated.

As shown in Figure 3, the orientations of 9-substituted anthracenes and pyrene molecules are dependent on host crystallinity, but only when the crystalline content is  $<$  ca.  $50\%$  before film stretching. As crystallinity is increased within this range, more chromophores can be deposited epitaxially along crystal surfaces and the average orientation improves. When

the crystalline content is  $<$  ca.  $50\%$  before stretching, the crystal surface area appears to be sufficiently large to dominate the partitioning with the amorphous regions. Additional increases in crystallinity and crystal surface area are not necessary for almost all of the chromophores to reside in the interfacial regions (at least at the concentrations where physical measurements are meaningful). Other factors, like frequency and lengths of branching and crystallite size, also must contribute to the specificity of orientation, but the degree of crystallinity appears to be the most important parameter for describing the relation between chromophore orientation and polyethylene morphology.

The anthryl molecule with a long substituent, **MeAuc**, is less dependent on crystallinity than the anthryl molecules with shorter substituents, **MeA** and **MeAac** (Figure 3). Apparently, interactions between the long alkyl substituent in **MeAuc** and nearby chains of the polymer matrix compete with the forces aligning the anthryl moiety on a polymer crystal surface, making it more difficult for the anthryl groups of **MeAuc** to respond to differences in their local environment.

**Effect of Temperature on Chromophore Orientation.** Solute alignment in stretched polyethylene films is known to increase as temperature is lowered from ambient to  $77$  K (liquid nitrogen).<sup>29</sup> Recently, a systematic study has shown that most of the increase takes place between ambient and ca.  $-20$  °C (i.e., near the glass transition of amorphous polyethylene chains), and correlates well with the improved polymer chain alignment in the interfacial regions.<sup>29</sup> Below the glass transition temperature, segmental chain motions necessary for chromophores such as anthryl and pyrenyl to reorient significantly are not possible.<sup>12</sup> However, our results with the 9-anthryl or 1-pyrenyl moieties doped in or covalently attached to polyolefinic films at both room temperature and ca.  $-30$  °C indicate that the reasons for the increases in the orientational factors are more complex, and depend on the nature of both the chromophores and the films.

As shown in Table 3, the orientation factors of **MeA** in **EPDM12** and **MeAac** in **PE37**, **PE46**, and **PE50** (stretched **LDPE** films) increase by  $13$ – $20\%$  between room temperature and  $-30$  °C. However, there is no corresponding change in  $K_z$  of **MeAac** in **PE68** and **PE74** (stretched **HDPE** films) or in  $K_z$  of **MeAuc** in any of the stretched films. These results suggest that the mobility and ordering of noncrystalline chains in the vicinity of the aromatic guest molecules, especially those in the interfacial regions, is affected between room temperature and the glass transition to a much greater extent in the **LDPE** films than in the **HDPE** ones. **HDPE** films have fewer branches and their chains are packed well even at room temperature.

On the basis of the  $K_z$  values in Tables 3 and 4, the tethers of the covalently attached 9-anthryl and 1-pyrenyl groups and the long 9-alkyl substituent on **MeAuc** must be “anchors” that make the orientations of the chromophores rather insensitive to environmental changes induced by temperature. The  $K_z$  of **MeA** and **PyH** in stretched **EPDM0** films remain ca.  $0.33$  at ambient temperature and  $-30$  °C due to the lack of crystallinity in the polymer matrix. However, the  $K_z$  of **EtPy** in stretched **PE37**–**PE74** films do increase somewhat and the orientation of **PyH** in stretched **EPDM12** increases by  $15\%$  when temperature is reduced. For reasons that are still being determined at this point, the  $K_z$  of the pyrenyl-containing molecules were not affected by temperature in the other **PE** films.

**Orientalional Distributions of Pyrene or 1-Pyrenyl Groups in Polyethylene Films.** The second-order orientation factor  $K_u$  reflects the average orientation of all chromophores in a film, but does not provide insights concerning their distribution. This information is available from the fourth-order orientation factor



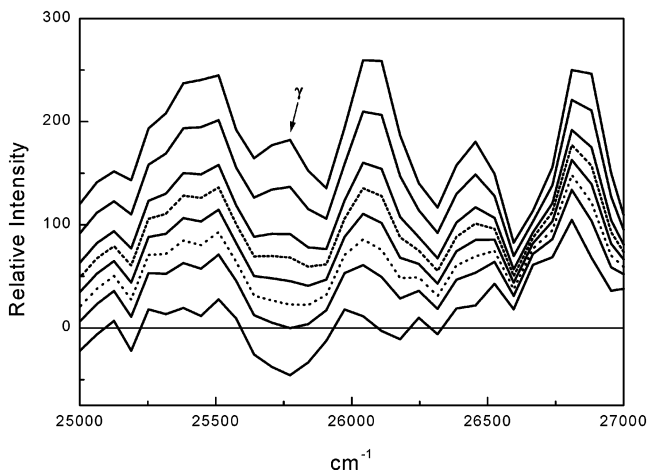


**Figure 4.** Stepwise reduction of  $I_{ZY} - [S_{ZY}(zz)/S_{ZZ}(zz)]I_{ZZ}$  to remove the  $z$ -polarized spectral feature  $\gamma$  in the fluorescence spectrum of stretched **PyH/PE46** at  $-54$  °C ( $[PyH] = 1.6$  mmol/kg). For the curves from top to bottom  $S_{ZY}(zz)/S_{ZZ}(zz) = 0.0, 0.1, 0.2, 0.25, 0.3, 0.35, 0.4,$  and  $0.5$ , respectively. The  $\gamma$  band disappears at  $S_{ZY}(zz)/S_{ZZ}(zz) = 0.3$  and the reduced spectra next to it (when  $S_{ZY}(zz)/S_{ZZ}(zz) = 0.25$  and  $0.35$ ) are dotted to indicate the critical region.

**TABLE 5: Orientation Parameters ( $L_{zz}$  and  $K_z^2$ ) of Pyrenyl Groups in Stretched PE Films at Subambient Temperatures**

film	[Pyrenyl] (mmol/kg)	$L_{zz}^{a,b}$	$K_z^2$ <sup>a</sup>
<b>PyH/PE46</b>	1.6	$0.33 \pm 0.07$	$0.27 \pm 0.02$
<b>PyH/PE74</b>	1.4	$0.39 \pm 0.10$	$0.34 \pm 0.02$
<b>EtPy/PE46</b>	1.2	$0.41 \pm 0.10$	$0.37 \pm 0.02$
<b>PyCH<sub>2</sub>-PE46</b>	2.2	$0.32 \pm 0.08$	$0.23 \pm 0.02$
<b>EtPy/PE74</b>	< 0.2	$0.37 \pm 0.10$	$0.35 \pm 0.02$
<b>PyCH<sub>2</sub>-PE74</b>	0.7	$0.34 \pm 0.08$	$0.26 \pm 0.02$

<sup>a</sup>  $K_z$  values from polarized UV/vis absorption spectra at  $-30 \pm 5$  °C;  $L_{zz}$  values from polarized fluorescence spectroscopy at  $-50 \pm 5$  °C. <sup>b</sup> Because the  $^1L_a$  absorption transition moment in 1-substituted pyrene is along the  $z'$  axis, the orientation factors  $L_{zz}$  for **EtPy** or **PyCH<sub>2</sub>-** are actually  $L_{z'z'}$ .

$L_{uv}$ . In a uniaxial system like stretched polyethylene,  $L_{uv} = \langle \cos^2(u,Z) \cos^2(v,Z) \rangle$ , where  $u$  and  $v$  are the directions of the excitation and emission transition moment, respectively.<sup>4e</sup> When  $u = v = z$ ,  $L_{uv} = L_{zz} = \langle \cos^2(z, Z) \cos^2(z, Z) \rangle$ . The closer are the values of  $L_{zz}$  and  $K_z^2$ , the narrower is the orientational distribution. In an ideal case, when all chromophores are oriented at the same angle with the molecular axis  $z$  relative to the stretching direction  $Z$ ,  $L_{zz} = K_z^2$ .<sup>4e</sup>

Polarized fluorescence spectra of the pyrenyl groups were measured to obtain  $L_{zz}$  at ca.  $-50$  °C, where reorientational motions during the rather long excited singlet state lifetime are inconsequential. Unfortunately, similar measurements could not be performed on the 9-anthryl groups.<sup>38</sup> Figure 4 shows the polarized fluorescence spectra of **PyH/PE46**. The  $\gamma$ -emission peak is  $z$ -polarized but overlaps partially with  $y$ -polarized fluorescence features.<sup>39</sup> The spectrum was "reduced" in a stepwise manner to separate the polarization components:<sup>39</sup> when the linear combination of  $I_{ZZ}$  and  $I_{ZY}$ ,  $I_{ZY} - [S_{ZY}(zz)/S_{ZZ}(zz)]I_{ZZ}$ , leads to the disappearance of the  $z$ -polarized  $\gamma$  band, eq 1 holds.

$$S_{ZY}(zz)/S_{ZZ}(zz) = (K_z - L_{zz})/2L_{zz} \quad (1)$$

The  $K_z$  values are from polarized UV absorption spectra at  $-30$  °C.<sup>40</sup> Thus,  $L_{zz}$  values for **PyH** or 1-pyrenyl groups have been calculated and compared with the corresponding  $K_z^2$  (Table 5). When the pyrenyl chromophores are doped in the polyethylene

films, the  $L_{zz}$  and  $K_z^2$  values are nearly the same and indicate a narrow distribution of orientations. The  $L_{zz} - K_z^2$  difference for **PyH/PE46** remains very small at several temperatures below the glass transition of the polymer (between  $-36$  and  $-60$  °C), and indicates an orientational distribution of pyrene like that reported in a stretched **LLDPE** film at 77 K.<sup>41</sup> However, when the pyrenyl chromophores are covalently attached, like in **PyCH<sub>2</sub>-PE46** and **PyCH<sub>2</sub>-PE74**, the differences between  $L_{zz}$  and  $K_z^2$  are large, suggesting a wider distribution of orientations.

## Discussion

**Distributions between Amorphous and Interfacial Sites and Orientational Distributions of Covalently Attached Aromatic Groups and Doped Aromatic Molecules in Polyethylene Films.** According to the "epitaxial deposition model," in a stretched film aromatic guest molecules may be distributed among sites in (a) the amorphous regions where the molecules are randomly oriented, (b) along the (110) faces of lamellar crystallites where their long molecular axes are oriented in the same direction as the polymer chains in the lamellae, and (c) on the (100) faces of crystallites where their long molecular axes are oriented perpendicularly to the molecules in (b).<sup>7c</sup> The measured value of  $K_z$  is the mean weighted average of the orientations experienced by molecules in the three environments:  $K_z = K_{za}\chi_a + K_{zb}\chi_b + K_{zc}\chi_c$ , where the sum of the mole fractions,  $\chi_i$ , is one and  $K_{zi}$  is the orientation factor for those molecules residing in site type  $i$ . For instance, acridine molecules have been reported to reside only in amorphous regions of *unstretched* polyethylene films (i.e.,  $\chi_a = 1$  and  $K_{za} = 0.33$ ), and their anisotropic orientation in *stretched* films is ascribed to a translocation of some molecules from amorphous sites to those on crystal surfaces ( $\chi_a = 0.56$  and  $\chi_b = 0.31-0.33$ ).<sup>7c</sup>

Since  $L_{zz} \approx K_z^2$  (the difference between  $L_{zz}$  and  $K_z^2$  is  $\leq 20\%$ ) when measured in our and other<sup>41</sup> stretched **LDPE** films, the chromophore orientational distribution of **PyH** must be intrinsically narrow; pyrene molecules align at a similar angle with respect to the direction of stretch in several types of **PE** films. It follows that the distribution of the  $\chi_i$  must be similar in these **PE** films as well and that  $\chi_b$  is very large (i.e., most **PyH** guests prefer to occupy sites along the (110) faces of lamellar crystallites in stretched **PE** films). In support of this hypothesis, pyrene molecules doped in **EPDM0**, a model polymer for the amorphous phase of **PE**, remain unoriented after stretching (so that  $\chi_a \approx 1$ ), even at ca.  $-30$  °C. If, like acridine, the pyrene molecules are only in the amorphous regions before film stretching, most (*unlike* acridine) must translocate to interfacial regions during film stretching.

Covalently attached chromophores are not able to translocate and must retain approximately the same regional distributions before and after film stretching. Therefore, they provide insights into the changes that occur to local amorphous as well as interfacial environments when films are stretched. As observed by others<sup>11</sup> and us, covalently attached anthryl and pyrenyl groups are *not* aligned *macroscopically* in *unstretched* polyethylene (i.e.,  $K_z = 0.33 \pm 0.02$ ), but develop a net macroscopic orientation *after* film stretching ( $K_z > 0.33$ ).

If  $\chi_a \approx 1$  for these attached chromophores in *unstretched* **PE** films, they must undergo rotational motions that do not require translocations to become oriented with respect to the laboratory frame *after stretching*. One way by which this may be accomplished is if the aromatic groups become aligned with polymer chains constituting nearby lateral crystal surfaces of newly formed crystallites. In this way, they can be deposited epitaxially and show a net macroscopic orientation. Alterna-

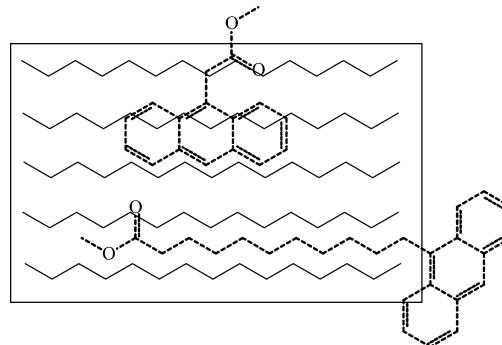
tively, a significant fraction of the covalently attached aromatic groups reside in interfacial sites, especially in environment b,<sup>7c</sup> before film stretching (i.e.,  $\chi_a \ll 1$ ). The aromatic groups along the (110) crystal faces are, in sum, disoriented before stretching because the polymer chains and crystals are not oriented with respect to a film axis, but they become oriented macroscopically to the extent that their crystallites are after stretching. We prefer this latter hypothesis for covalently attached groups because it seems unreasonable that the various types of stretched PE films with different crystallinities in Table 4 would provide very similar large  $K_z$  values for **PyCH<sub>2</sub>-** groups and that  $K_z$  would be 0.33 in a completely amorphous stretched film if  $\chi_a \approx 1$  before stretching in all cases.

It follows from the results with covalently attached groups that a significant mole fraction of *doped* molecules also reside in interfacial sites prior to film stretching. Our results strongly support this contention. First, if doped aromatic chromophores have a preference for residing near polymer crystal surfaces after stretching, they should prefer to do so before stretching as well. For instance, reductions in hole free volume upon film stretching, a factor that might force molecules in interfacial sites to move to amorphous ones, are small with respect to the van der Waals volumes of anthryl and pyrenyl groups.<sup>42</sup> The same preference would also promote translocation of aromatic dopants, when they are not covalently attached, from amorphous regions to polymer crystal surfaces during stretching because of the increased crystal surface area after stretching.<sup>7c</sup> Second, from studies of the thermal isomerization of azobenzenyl groups covalently attached to interior sites of stretched PE films, we estimate that at least 70% of the azobenzenyl groups are in interfacial regions.<sup>43</sup> This preference can be traced to the site distribution of one doped molecule, **DBTO**, since it determines the sites where hydroxylation (and subsequent covalent attachment of azobenzenyl groups through esterification) occurs.<sup>28</sup> Since the same attachment method has been employed here with the 9-anthryl groups, their locations within the PE films should be like that of the azobenzenyl groups.

The breadths of the orientational distributions of **EtPy** and pyrene in **LDPE** are similar; in both cases, the differences between  $L_{zz}$  and  $K_z^2$  are < 20% of each value. However, the distribution of orientations is much larger for the covalently attached analogue of **EtPy**, **PyCH<sub>2</sub>-** groups, where the difference between  $L_{zz}$  and  $K_z^2$  is ca. 40%. Although covalently attached and doped chromophores may be distributed similarly among the three potential site types before stretching, they need not be after stretching. As a result of the freedom to diffuse translationally after film stretching,  $\chi_b$  of the doped molecules is expected to be larger than that of the covalently attached groups in stretched films.

**Are Interactions between Aromatic Groups and a Polymer Matrix or Translocation More Important to Orientation?** Although **MeA**, **MeAac**, and **MeAuc** are all free to translocate from amorphous regions to crystal surfaces during film stretching, **MeAuc** is oriented less well than **MeA** or **MeAac** in **PE37-PE74** films (Table 3). Interactions between the substituent at the 9-position of anthryl and neighboring polyethylene chains must contribute to the overall molecular alignments. The long alkyl chain of **MeAuc** can interact via favorable, dispersive London contacts with neighboring polyethylene chains, decreasing the mole fraction and/or specificity of adsorption of the anthryl group on crystal surfaces. The strong dispersion forces between undecanoyl groups and surrounding polymer chains, as well as the oblique angle they make with the long axis of the aromatic part, may impede anthryl groups from aligning as

**SCHEME 3: A Cartoon Representation of the Hypothetical Preferred Orientation of Anthryl with a Short (MeAac) or a Long (MeAuc) Substituent on a Lateral Crystal Surface of PE.**



they would in **MeA** or **MeAac**; as shown in Scheme 3, the aromatic and alkyl parts interact with their polymer environment at “cross-purposes” with respect to alignment. Thus, both the orientation and the site distribution of anthryl groups in stretched polyethylene films may vary with the length of a 9-alkyl substituent. Similarly, the conformational constraints imposed by the methylene that links 1-pyrenyl groups to polyethylene chains may be the reason that they are not aligned as well as the unattached **EtPy** molecules.

Covalently attached anthryl or pyrenyl groups cannot translocate over large distances (i.e., from amorphous to interfacial regions) during film stretching. The fact that they are partially oriented by stretching indicates that translocation is not necessary for orientation to occur. Furthermore, even though the covalently attached anthryl groups with short tethers, **ACH<sub>2</sub>-** and **Aac-**, orient less well than their doped analogues, **MeA** and **MeAac**, the covalently attached 9-anthryl group with a long tether, **Auc-**, is oriented like its doped analogue, **MeAuc**, for reasons discussed above. For example,  $K_z = 0.58$  for **MeA/PE46**<sup>11</sup> and **MeAac/PE46**, but  $= 0.47 \pm 0.02$  for **ACH<sub>2</sub>-PE46**, **Aac-PE46**, and **MeAuc/PE46** (Table 3). This indicates that translocation is less important to orientation than how the aromatic group (and its substituent) interact with surrounding polymer chains. Only when the aromatic group is free of unfavorable interactions with the polymer matrix, like those that may be imposed by a covalent linkage or a long alkyl substituent, can it orient to the maximum extent allowed by the polymer matrix.

**Conclusions**

Our results with **EPDM0** films demonstrate unambiguously the absence of macroscopic orientation of guest molecules in amorphous regions of stretched polyolefinic films; *crystallite surfaces are necessary for nonrandom orientation*. These results strongly support the “epitaxial deposition model”.<sup>7c</sup>

Comparisons of linear polarizations between covalently attached aromatic groups and doped aromatic molecules with substituents/tethers of different lengths demonstrate that the nature and specificity of interactions of the aromatic groups and their substituents with neighboring polyolefinic chains determine the ease of translocation and orientation. Strong van der Waals interactions, including London dispersion forces between polyolefinic chains and a long alkyl substituent of a noncovalently attached aromatic group, or spatial constraints applied through covalent attachment, hinder translocation and epitaxial deposition of aromatic molecules on crystal surfaces of the host matrix. These findings are consistent with and are expansions of the “polarizability/shape model”.<sup>6</sup>

The fact that covalently attached aromatic groups are partially oriented in the stretched films suggests that, while stretching-induced net translocation of aromatic molecules from amorphous to interfacial regions takes place when molecules are doped into the films, it is not necessary for orientation to occur; aromatic groups such as pyrenyl and anthryl prefer to reside in interfacial sites even before film stretching. In addition, a long-suspected dependence of molecular orientation on film morphology has been verified for the first time by using polyethylene films with a wide range of crystallinities. The dependence on crystallinity is strong when the crystalline content is relatively low, < ca. 50%. No dependence of orientation on chromophore concentration has been found within the limited range examined, but it must exist for several reasons at higher concentrations.

These data, *in toto*, demonstrate that the orientation factors reported for one molecule in different laboratories need not be the same if the stretched polyethylene matrix is different. We offer these results as a caveat that orientational factors are most useful when they are compared for different guest molecules within one polymer or for one guest molecule within different polymers. The information that can be gleaned in the two cases is subtly different, and the additional possibility of investigating similar species that are covalently attached to the polymer matrix opens possibilities for detailed investigations of polymer microstructure.

**Acknowledgment.** We are grateful to Ms. Becky Decker of R. T. Vanderbilt Company (Murray, Kentucky) for supplying the EPDM materials and to Ms. Nancy Richter of the Baytown Polymers Center of Exxon (Texas), Mr. Mario Lutterotti of Dupont of Canada (Ontario, Canada), and Polialden Petroquímica of Brazil (through Prof. Teresa Atvars) for the polyethylene films. We thank Prof. Erik Thulstrup for several helpful suggestions and discussions, Mr. Jingsong Huang and Prof. Miklos Kertesz for their help with the calculations, and Dr. Chuping Luo for assistance with the low-temperature polarization measurements. The National Science Foundation is gratefully acknowledged for its support of this work.

**Supporting Information Available:** Two tables of fluorescence decay constants and relative preexponential factors for an **Auc-PE46** film and for **PyCH<sub>2</sub>-PE** films, UV/vis absorption spectra showing the course of the 1-pyrenyl attachment process, excitation and emission spectra of an **Auc-PE46** film. This material is available free of charge via the Internet at <http://pubs.acs.org>.

## References and Notes

- Jablonski, A. *Nature* **1934**, 133, 140.
- For a comprehensive review, see: Thulstrup, E. W.; Michl, J. *J. Phys. Chem.* **1980**, 84, 82.
- For examples, see: (a) Konwerska-Hrabowska, J.; Chantry, G. W.; Nicol, E. A. *J. Infrared Millimeter Waves* **1981**, 2, 1135. (b) Radziszewski, J. G.; Michl, J. *J. Phys. Chem.* **1981**, 85, 2934.
- See, for example: (a) Thulstrup, E. W.; Eggers, J. H. *Chem. Phys. Lett.* **1968**, 1, 690. (b) Thulstrup, E. W.; Michl, J.; Eggers, J. H. *J. Phys. Chem.* **1970**, 74, 3868. (c) Michl, J.; Thulstrup, E. W. *Acc. Chem. Res.* **1987**, 20, 192. (d) Michl, J.; Thulstrup, E. W. *Spectroscopy with Polarized Light. Solute Alignment by Photoselection in Liquid Crystals, Polymers and Membranes*; VCH: New York, 1986. (e) Thulstrup, E. W.; Michl, J. *Elementary Polarization Spectroscopy*; VCH: New York, 1989.
- Thulstrup, E. W.; Michl, J. *J. Am. Chem. Soc.* **1982**, 104, 5594.
- Konwerska-Hrabowska, J. *Appl. Spectrosc.* **1985**, 39, 434.
- (a) Jang, Y. T.; Phillips, P. J.; Thulstrup, E. W. *Chem. Phys. Lett.* **1982**, 93, 66. (b) Parikh, D.; Phillips, P. J. *J. Chem. Phys.* **1985**, 83, 1948. (c) Phillips, P. J. *Chem. Rev.* **1990**, 90, 425.
- Long, T. M.; Swager, T. M. *Adv. Mater.* **2001**, 13, 601.
- Konwerska-Hrabowska, J.; Eggers, J. H. *Spectrosc. Lett.* **1977**, 10, 441.
- (a) Yogev, A.; Margulies, L.; Amar, D.; Mazur, Y. *J. Am. Chem. Soc.* **1969**, 91, 4558. (b) Yogev, A.; Riboid, J.; Marero, J.; Mazur, Y. *J. Am. Chem. Soc.* **1969**, 91, 4559. (c) Margulies, L.; Yogev, A. *Chem. Phys.* **1978**, 27, 89.
- He, Z.; Hammond, G. S.; Weiss, R. G. *Macromolecules* **1992**, 25, 1568.
- Talhavini, M.; Atvars, T. D. Z.; Schurr, O.; Weiss, R. G. *Polymer* **1998**, 39, 3221.
- Materials Data Inc., Release 5.0.35 (SPS), Livermore, CA.
- Zimmerman, O. E.; Cui, C.; Wang, X.; Atvars, T. D. Z.; Weiss, R. G. *Polymer* **1998**, 39, 1177.
- Kluge, R.; Schulc, M.; Liebsh, S. *Tetrahedron* **1996**, 52, 5773.
- Ho, T.-L.; Wong, C. M. *Synthesis* **1972**, 562.
- Huang, M. L. *J. Am. Chem. Soc.* **1949**, 71, 3301.
- Perrin, D. D.; Amarego, W. L. *Purification of Laboratory Chemicals*, 3rd ed.; Pergamon: New York, 1988; p 267.
- Zimmerman, O. E.; Weiss, R. G. *J. Phys. Chem. A* **1999**, 103, 9794.
- Joseph, E.; Radt, F., Eds. *Elsevier's Encyclopedia of Organic Chemistry*; Series III, Vol. 14; Elsevier: New York, 1940; p 379.
- Jamison, T. F.; Lubell, W. D.; Dener, J. M.; Krisché, M. J.; Rapoport, H. In *Organic Syntheses, Collective Volume IX*; Freeman, J. P., Ed.; Wiley: New York, 1998; pp 103–106.
- Ciganek, E. *J. Org. Chem.* **1980**, 45, 1497.
- Wiesler, W. T.; Nakanishi, K. *J. Am. Chem. Soc.* **1990**, 112, 5574.
- Acton, N.; Berliner, E. *J. Am. Chem. Soc.* **1964**, 86, 3312.
- Boyer, J. H.; Schoen, W. In *Organic Syntheses, Collective Volume IV*; Rabjohn, N., Ed.; Wiley: New York, 1967; p 532.
- (a) Miyaura, N.; Ishiyama, T.; Ishikawa, M.; Suzuki, A. *Tetrahedron Lett.* **1986**, 27, 6369. (b) Esteban, G.; López-Sánchez, M. A.; Martínez, M. E.; Plumet, J. *Tetrahedron* **1998**, 54, 197.
- Silva, S.; Olea, A. F.; Thomas, J. K. *Photochem. Photobiol.* **1991**, 54, 511.
- Wang, C.; Weiss, R. G. *Macromolecules* **1999**, 32, 7032.
- Steenstrup, F. R.; Christensen, K.; Svane, C.; Thulstrup, E. W. *J. Mol. Struct.* **1997**, 408/409, 139.
- Hyperchem 5.1, Hypercube Inc.: Gainesville, FL, 1997.
- (a) Ravve, A. *Principles of Polymer Chemistry*; Plenum Press: New York, 1995; p 223. (b) Lazár, M.; Rychlxc6, J. *Adv. Polym. Sci.* **1992**, 102, 190. (c) Schnabel, W. *Polymer Degradation: Principles and Practical Applications*; Hanser: Wien, 1981; p 17.
- Gregory, D. D.; Wan, Z.; Jenks, W. S. *J. Am. Chem. Soc.* **1997**, 119, 94.
- Zimmerman, O. E.; Weiss, R. G. *J. Phys. Chem. A* **1998**, 102, 5364.
- Gilbert, A.; Baggott, J. *Essentials of Molecular Photochemistry*; CRC Press: Boca Raton, FL, 1991; p 168.
- Michl, J.; Thulstrup, E. W.; Eggers, J. H. *Ber. Bunsen-Ges. Phys. Chem.* **1974**, 78, 575.
- (a) Ham, J. S. *J. Chem. Phys.* **1953**, 21, 756. (b) Platt, J. R. *J. Mol. Spectrosc.* **1962**, 9, 288.
- Konwerska-Hrabowska, J. *Appl. Spectrosc.* **1985**, 39, 976.
- Our attempts to obtain  $L_{zz}$  for anthracene were frustrated by the very low concentration ( $10^{-5}$  M) needed in order to avoid depolarization from chromophore–chromophore radiative energy transfer. A  $10^{-4}$  M sample showed a smaller (0, 0) emission band than (0, 1) band, due to radiative energy transfer between the chromophores. While the  $10^{-5}$  M concentration sample had reasonably strong emission signals *before* stretching, it exhibited a very poor signal-to-noise ratio *after* stretching, even in the absence of a polarizer. Measurement of the fluorescence spectra in the presence of two polarizers was not possible.
- Langkilde, F. W.; Thulstrup, E. W.; Michl, J. *J. Chem. Phys.* **1983**, 78, 3372.
- The difference between  $K_z$  values at  $-30$  °C and  $-50$  °C is very small.<sup>29</sup>
- Langkilde, F. W.; Gisin, M.; Thulstrup, E. W.; Michl, J. *J. Phys. Chem.* **1983**, 87, 2901.
- Gu, W.; Hill, A. J.; Wang, X.; Cui, C.; Weiss, R. G. *Macromolecules* **2000**, 33, 7801.
- Wang, C.; Weiss, R. G. *Macromolecules* **2003**, 36, 3833.